Ciencia y Tecnología, 36(1): 1-22, 2020
ISSN: 2215-5708

THE HYDROGEN ATOM IN MOMENTUM SPACE

El ÁTOMO DE HIDRÓGENO EN EL ESPACIO DE MOMENTOS

*J. F. Ogilvie**

Escuela de Química, Universidad de Costa Rica, Ciudad Universitaria Rodrigo Facio,
San Pedro de Montes de Oca, San José, Costa Rica 11501-2060,
Centre for Experimental and Constructive Mathematics, Department of Mathematics,
Simon Fraser University, 8888 University Drive, Burnaby, British Columbia V5A 1S6 Canada,
Institute of Quantum Physics, Irkutsk National Research Technical University,
83 Lemontov Street, Irkutsk 664074, Russian Federation

Recebido 2019 octubre; *aceptado 2019 diciembre*

Abstract

To complement the existing descriptions of amplitude functions for the hydrogen atom in the coordinate representation in various systems, we present all known and well characterised amplitude functions in the corresponding momentum representation, specifically according to the treatments of Podolsky and Pauling on transformation from spherical polar coordinates, of Klein on a transformation analogous to that from paraboloidal coordinates, and of Lombardi on transformations from both spherical polar and paraboloidal coordinates. Figures depicting surfaces of the functions in their real and imaginary parts or their squares illustrate the diversity of shapes of these surfaces according to the various momentum variables.

Resumen

Para complementar la descripción de las funciones de amplitud existentes para el átomo de hidrógeno, en las representaciones de varios sistemas de coordenadas, se presentan todas las funciones de amplitud conocidas y caracterizadas. Específicamente, se muestran los tratamientos de Podolsky y Pauling transformando a partir de las coordenadas polares esféricas, las de Klein, transformadas a partir de coordenadas paraboloides, y las de Lombardi, transformadas a partir de coordenadas polares esféricas y paraboloides. Las imágenes que representan las superficies de las funciones en sus partes reales e imaginarias o sus funciones cuadradas, muestran la diversidad de las formas de estas superficies según las diversas variables en el espacio de momentos.

Key words: wave mechanics, momentum representation, Fourier transformation, coordinate systems

Palabras clave: mecánica de ondas, representación de espacio de momentos, transformación Fourier, sistemas de coordenadas

I INTRODUCTION

The hydrogen atom was the subject of treatments in quantum mechanics within two of its first three formulations. Pauli first applied a symbolic approach in which commutation relations were imposed; Schroedinger's wave mechanics then relied on a fact that a coordinate quantity and its derivative fail to commute -- $x\,\mathrm{d}y/\mathrm{d}x \neq \mathrm{d}(xy)/\mathrm{d}x$. This commutation condition was recognised, and named, by Dirac as the distinguishing characteristic of quantum mechanics, which is a collection of at least thirteen methods of calculation, or algorithms, that are applicable to systems on an atomic scale; the original method was matrix mechanics but Heisenberg could not devise a procedure to encompass the coulombic potential energy in his attempted solution of the hydrogen atom. Ever since Balmer derived, purely numerologically, his intriguing formula for the wave lengths of four lines in the visible spectrum attributed to atomic hydrogen, physicists have sought a theoretical approach to rationalise the revolutionary status of that formula: it contains a parameter that assumes only integer values; a discrete nature is hence implied for the internal energies accessible to an atom in a manner unfamiliar in traditional physics.

* corresponding author: ogilvie@cecm.sfu.ca

When Schroedinger (1926) published his four renowned papers that introduced wave mechanics, the community of physicists so appreciated this approach based on the solution of partial-differential equations that their interest in a development of alternative methods of quantum mechanics greatly waned. In the first of those papers Schroedinger solved his equation independent of time to generate the discrete energies of a hydrogen atom in bound states and produced amplitude functions in spherical polar coordinates; although this work had significant novelty, the energy formula was already known to be inaccurate, because the distinct features in the Balmer series were discovered to be not single lines but multiplets, and the derived amplitude functions were clearly artefacts of that particular solution. The second paper presented the solutions to a few formal problems, including a quadratic harmonic oscillator and a rigid rotor. The third paper was, in contrast, a monumental achievement because Schroedinger, in solving the hydrogen atom in paraboloidal coordinates, succeeded in calculating accurately not only the frequencies but also the intensities and polarisations of the spectral lines under the Stark effect. Heisenberg had previously stated that the observable properties of an atom or molecule are the frequencies and intensities of its spectral lines. The fourth paper was concerned primarily with the solution of an equation incorporating a dependence on time. In all these cases the kinetic energy of the electron in a hydrogen atom was treated in terms of a laplacian operator that resulted from momentum being represented as a derivative of a coordinate; for instance $p_x \rightarrow -\mathbf{i}\ \hbar\ \mathrm{d}/\mathrm{d}x$ in cartesian coordinates, in which $\mathbf{i} = \sqrt{-1}$ and $\hbar$ denotes the Dirac constant, or Planck constant h divided by $2\ \pi$. Mathematicians and physicists eventually recognised that the Schroedinger partial-differential equation for the hydrogen atom was solvable, through a separation of the spatial variables to yield ordinary-differential equations in coordinates in a manner that Schroedinger himself extolled in his third seminal article, in four systems in total -- ellipsoidal and spheroconical coordinates in addition to the original spherical polar and paraboloidal systems (Kalnins et alii, 1976).

One property involved in achieving Schroedinger's solutions that differs from a treatment in matrix mechanics, for instance, is a necessity to transform a mechanical variable, either a position or momentum for instance, into a differential operator of the other mechanical variable, either momentum or position respectively. That transformation involves the coordinate being replaced by a derivative with respect to momentum, for instance either $x \rightarrow -\mathbf{i}\ \hbar\ \mathrm{d}/\mathrm{d}p_x$ or $p_x \rightarrow \mathbf{i}\ \hbar\ \mathrm{d}/\mathrm{d}x$, all in cartesian coordinates. As a fundamental condition according to Schroedinger's approach, an application of either the momentum representation or the coordinate representation must yield the same result for an observable property in the form of an expectation value, such as the accessible internal energies of a system under consideration. There must hence exist solutions to the Schroedinger equation for the hydrogen atom in momentum variables that are equivalent to the corresponding solutions in coordinate variables for every purpose. In this article we present and illustrate these solutions in momentum space.

II. FUNCTIONS OF PODOLSKY AND PAULING, OF HYLLERAAS AND OF FOCK

Weyl (1927) stated first an accomplishment of a derivation of momentum eigenfunctions as a prospective solution for an integral equation for the hydrogen atom, but that claim was disputed by Podolsky and Pauling (1929); as an associate of Schroedinger in Zurich, Weyl was likely the first to state explicitly that the relation between amplitude functions in coordinate and momentum spaces might takes the form of a Fourier transformation. Podolsky (1928) recognised subsequently the essential validity of Dirac's replacement of each momentum variable η_r, conjugate to coordinate variable ξ_r, by its differential operator, $\eta_r \rightarrow -\mathbf{i}\ \hbar\ \mathrm{d}/\mathrm{d}\xi_r$; the crucial condition here is that *conjugacy* between the variables in the separate sets, which precedes an application of a Fourier transformation between the conjugate variables. When Podolsky worked subsequently with Pauling (1929) to derive "the momentum distribution in hydrogen-like atoms", Pauling apparently perverted Podolsky into the use of momentum variables as $P(p_r)$, $\Theta(\theta_p)$, $\Phi(\phi_p)$ that failed to conform to those essential conjugacy conditions. p_r denotes the radial component having the magnitude of the momentum vector but is a scalar quantity, $p_r = (p_x^2 + p_y^2 + p_z^2)^{½}$, with domain 0 ... ∞; its associated angular coordinates are θ_p and ϕ_p, of domains $0..\pi$ and $0..2\pi$ respectively, referred to the same cartesian axes as the position coordinates. Not only did those angular-momentum variables fail to obey that conjugacy property with respective coordinate variables θ, ϕ in the spherical polar system, contrary

to Podolsky's previously stated and correct understanding, but also they were effectively not even subjected to a Fourier transformation. The momentum amplitude functions derived by Podolsky and Pauling (1929) are expressible in this form, generated with *Maple* symbolic mathematical software,

$$\chi_{k,\,l,\,m}(p_r, \theta_p, \phi_p) = -2\,\mathbf{e}^{(i\,m\,\phi_p)}\sqrt{\frac{(2\,l+1)\,(l-|m|)!\,k!}{(l+|m|)!\,(k+2\,l+1)!}}\,(-4\,i\,n\,p_r)^l\,l!\,n^2\,(Z\,p_0)^{(5/2+l)}$$
$$\mathrm{P}(l,|m|,\cos(\theta_p))\,\mathrm{C}\left(k, l+1, \frac{-Z^2\,{p_0}^2 + n^2\,{p_r}^2}{Z^2\,{p_0}^2 + n^2\,{p_r}^2}\right) \Big/ \left(\pi\,(Z^2\,{p_0}^2 + n^2\,{p_r}^2)^{(l+2)}\right)$$

in which appear associated Legendre functions P of the first kind and Gegenbauer (ultraspherical) functions C; these amplitude functions are proved to be normalised and orthogonal. The angular factors P in terms of $\cos(\theta_p)$ and $\mathbf{e}^{(i\,m\,\phi_p)}$ have exactly the same forms as their presence in the amplitude functions in coordinate space, proving a lack of Fourier transformation, whereas the C functions might constitute an acceptable transform of radial function R(r) in spherical polar coordinates because a transform of an exponential function, of form $\mathbf{e}^{(-r)}$ multiplied by a polynomial in r in the coordinate representation, yields on Fourier transformation a function with an argument in a form resembling a lorentzian formula, $\frac{1}{1+p^2}$. That equation contains also the atomic unit of momentum, $p_0 = \hbar/a_0$ with Bohr radius a_0. Three quantum numbers k, l, m appear with the same meanings as in the solutions in spherical polar coordinates; explicitly, k indicates the number of radial nodes of P(p_r), with energy quantum number $n = k + l + 1$, whereas l and m specify the numbers of angular nodes. Although the resulting amplitude functions might appear to be useful for the calculation of various expectation values $\langle p^n \rangle$, they can not be considered to be truly expressed in the momentum representation, even before the falsity of the total transformation was recognised. In fact, even though $\langle p^2 \rangle$ calculated with the above amplitude functions yields a correct value, values of $\langle p^n \rangle$ for $n \neq 2$ are incorrect, as are expectation values of radial distance, $\langle r^n \rangle$, for $n \neq 2$. Plots of surfaces of these functions in momentum space at a selected value of ψ_p have, necessarily, exactly the same shapes and relative sizes, for given energy quantum number n, as their counterparts in spherical polar coordinate space, except that the figures contract with increasing n rather than expand as in coordinate space.We present just one figure, for $\chi_{1,1,0}(p_x,p_y,p_z)$, to illustrate a momentum amplitude function as a surface of constant momentum amplitude χ selected such that the volume within contains about 0.99 of the total momentum density; a similar criterion is applied in plots of other momentum amplitude functions to follow. The axes are the cartesian components of momentum in units of p_0. Comparison of this figure with a corresponding plot of $\psi_{1,1,0}(r,\theta,\phi)$, likewise in a frame of cartesian axes, indicates an identical shape and geometric characteristics.

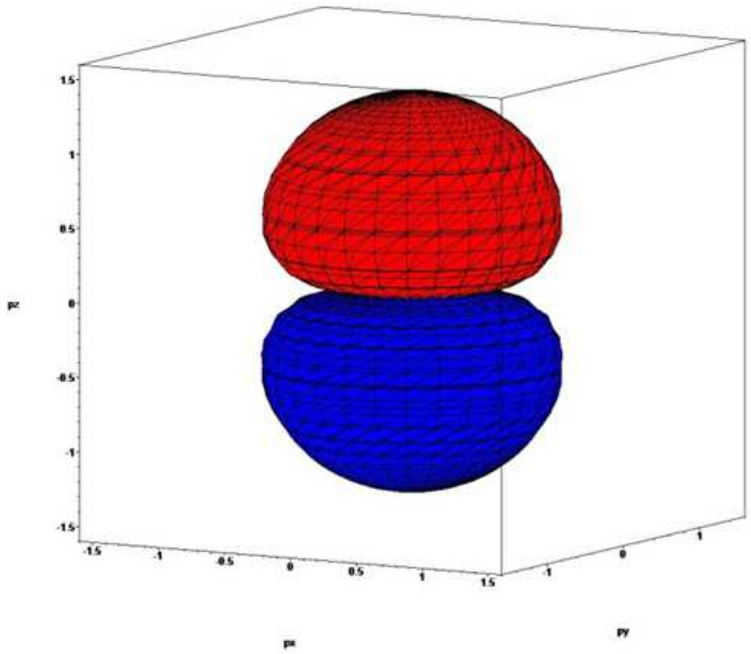

Figure 1. Surface of $\chi_{1,1,0}$ within a frame of cartesian components (p_x,p_y,p_z) of momentum; these components are in units divided by p_0, the atomic unit of momentum.

A practical approach to derive the amplitude functions for the hydrogen atom would seem to involve the direct solution of the appropriate differential Schroedinger equation in momentum space in terms of momentum variables; because the coulombic potential energy is proportional to r^{-1}, which causes complications in the replacement of r by a differential operator, such an equation is difficult to handle. An alternative approach involves rewriting the Schroedinger equation in the form of an integral equation in momentum space; although this scheme is also difficult to implement, it was undertaken by Hylleraas (1932), who generated the following formula for the amplitude function in momentum space, not normalised, containing Legendre functions for both variables p_r and θ_p, apparently accepting uncritically the angular parts proffered by Podolsky and Pauling (1929).

$$\chi_{n,\,l,\,m}(p_r,\,\theta_p,\,\phi_p) = \frac{p_r\,{p_0}^3\,\mathrm{P}\left(n+\frac{1}{2},\,l+\frac{1}{2},\,\frac{n^2\,{p_r}^2-{p_0}^2}{n^2\,{p_r}^2+{p_0}^2}\right)\mathrm{P}(l,\,m,\,\theta_p)\,\mathbf{e}^{(i\,m\,\phi_p)}}{\left(\frac{n^2\,{p_r}^2+{p_0}^2}{{p_0}^2}\right)^{l}\,(n^2\,{p_r}^2+{p_0}^2)^2}$$

Fock (1935) adopted an integral-equation approach to derive the eigenfunctions of the total momentum variable (p_r). He recognized that, if r had momentum-space analogue $-\boldsymbol{i}\,\hbar\,\mathrm{d}/\mathrm{d}p_r$, the inverse operator r^{-1} associated with the coulombic potential energy should be expressed as an integral operator. To solve this integral equation containing electronic mass μ,

$${p_r}^2\,\chi(p_r) - \left(\frac{\mu\,Z\,e^2\,h}{\pi^2}\int\frac{\chi(p_{r*})}{|p_r-p_{r*}|^2}\,dp_{r*}\right) = 2\,\mu\,E\,\chi(p_r)$$

Fock resorted to a four-dimensional scheme of hyperspherical polar coordinates, obtaining

$$\chi_{n,l,m}(\alpha,\theta,\phi) = \Pi_l(n,\alpha)\, Y_{l,m}(\theta,\phi)$$

in which radial function $\Pi_l(n,\alpha)$ that appears as a product with spherical harmonics, $Y_{l,m}(\theta,\phi)$, as in preceding work, was not elaborated explicitly. Therein angles α, θ, ϕ are spherical coordinates of a point on a hypersphere, but angles θ and ϕ are equally ordinary spherical coordinates characterizing the momentum direction. On projection back to three-dimensional space, he apparently recovered the results of Hylleraas (1932).

III FUNCTIONS OF KLEIN

After that moderate activity during the first decade after the origin of wave mechanics, no further pertinent development occurred until another three decades had elapsed. Klein (1966) solved the amplitude functions in momentum space in what he called toroidal coordinates, but these correspond to cylindrical coordinates of Kalnins et alii (1976). The relations between cartesian coordinates x, y, z and toroidal coordinates ξ, η, ϕ follow:

$$x = \frac{a\,\sinh(\eta)\cos(\phi)}{\cosh(\eta)-\cos(\xi)} \qquad y = \frac{a\,\sinh(\eta)\sin(\phi)}{\cosh(\eta)-\cos(\xi)} \qquad z = \frac{a\,\sin(\xi)}{\cosh(\eta)-\cos(\xi)}$$

Figures 2, 3 and 4 illustrate surfaces of constant ξ, η and ϕ in these toroidal coordinates, respectively. A surface of constant $\xi = ½\,\pi$ has the shape of a finite double cylinder joined at the top. A surface of constant $\eta = ½\,\pi$ has the shape of a dome, closed at the top, or perhaps a paraboloid opening downward. In contrast, the surface of constant $\phi = 0$ comprises one plane perpendicular to axis p_y. In all cases the surfaces are generated in toroidal coordinates but *Maple* software translates the figure into cartesian coordinates p_x, p_y, p_z for conventional viewing. We expect accordingly that amplitude functions in these momentum coordinates comprise domes, tori and planes in various combinations.

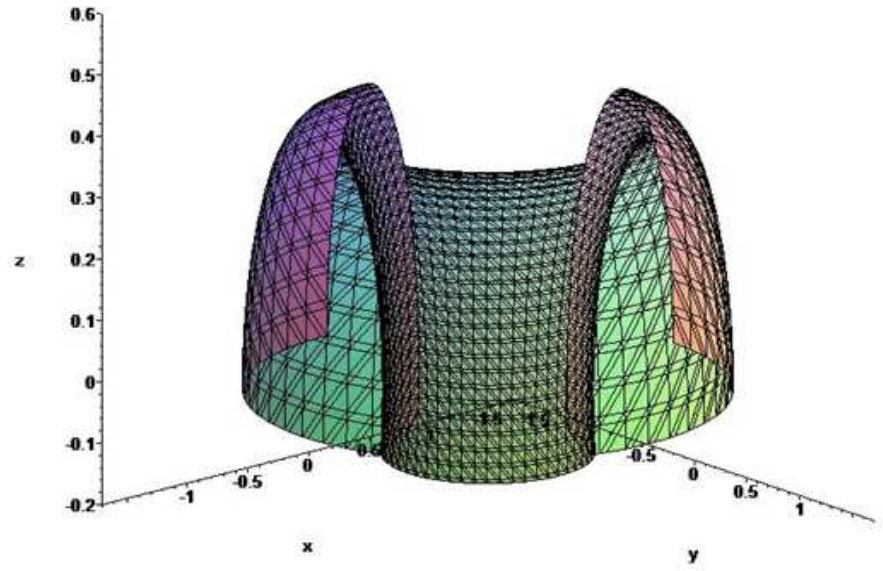

Figure 2. Surface of constant $\xi = ½\,\pi$ in toroidal coordinates translated to cartesian coordinates, cut open to exhibit the internal structure

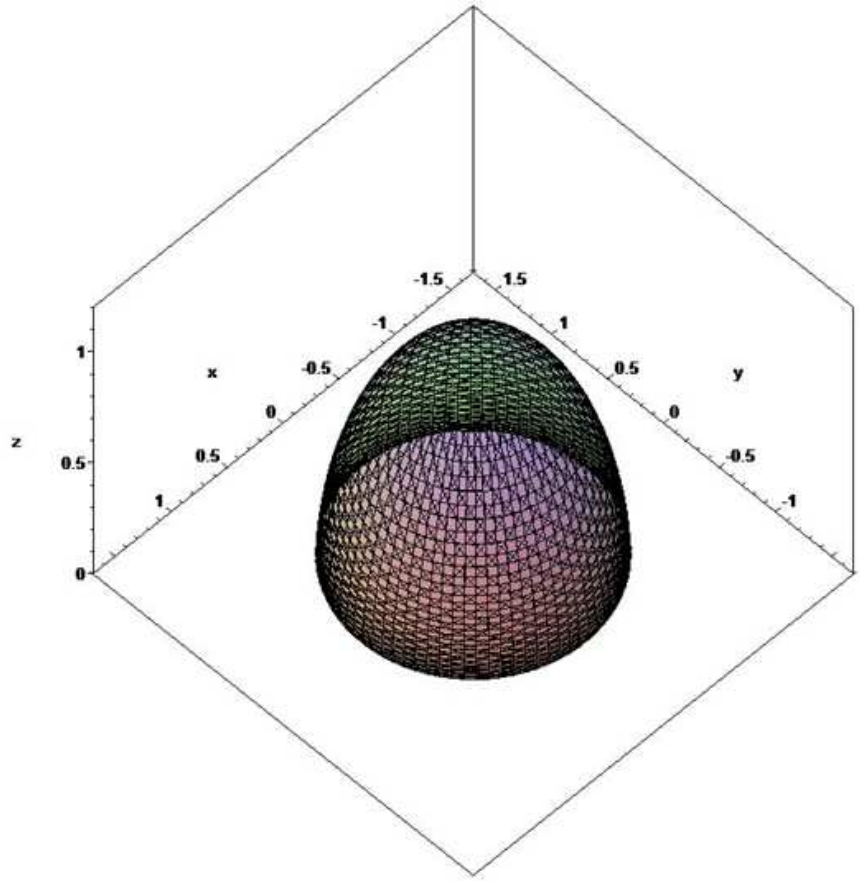

Figure 3. Surface of constant $\eta = \frac{1}{2}\pi$ in toroidal coordinates translated to cartesian coordinates

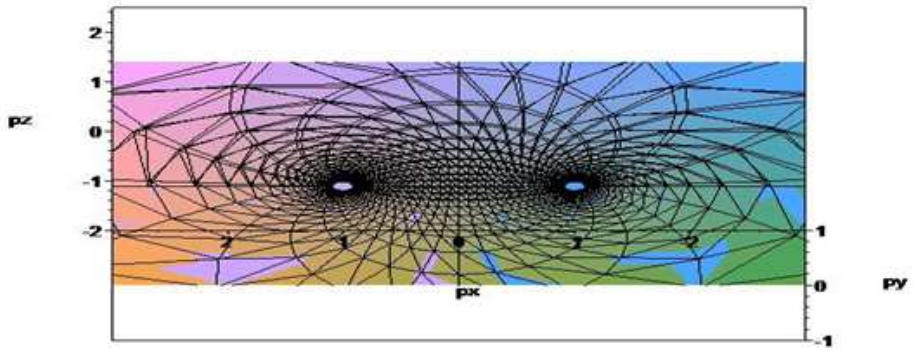

Figure 4. Surface of constant $\phi = \frac{1}{2}\pi$ in toroidal coordinates translated to cartesian coordinates, showing a planar surface with contours around two foci

Klein's function for momentum amplitude, with symbolic normalisation factor N and containing Jacobi polynomials P as a function of η, is expressible as

$$\chi_{k,\,l,\,m}(\xi, \eta, \phi) = \frac{1}{4}$$

$$N\,\mathrm{P}(l, k+m+1, k+1, \mathrm{sech}(\eta)^2)\,\tanh(\eta)^m\,\mathrm{sech}(\eta)^k\,\mathbf{e}^{(i\,k\,\xi)}\,\mathbf{e}^{(i\,m\,\phi)}\left(1 - \frac{\cos(\xi)}{\cosh(\eta)}\right)^2$$

Parameters k, l, m that appear in this equation are quantum numbers as arguments of the Jacobi function and as exponents of hyperbolic trigonometric functions tanh and sech, but their meanings differ from those of quantum numbers in spherical polar coordinates denoted with the same symbols; in this case energy quantum number $n = k + 2\,l + m + 1$.

We proceed to display figures of these momentum amplitude functions, never previously reported. The first function, unnormalised, is for the ground state of the hydrogen atom:

$$\chi_{1,\,0,\,0}(\eta, \xi, \phi) = \frac{\mathbf{e}^{(i\,\xi)}\,(\cosh(\eta) - \cos(\xi))^2}{4\,\cosh(\eta)^3}$$

All these functions are complex, even without exponential term $\mathbf{e}^{im\phi}$ for ϕ when $m \neq 0$, because of the exponential term $\mathbf{e}^{i\xi}$ for ξ. For this reason we display separately surfaces of the real and imaginary parts of $\chi_{1,0,0}$ and its square, $|\chi_{1,0,0}|^2$, in figures 5, 6 and 7. In all cases of these surfaces, a value of χ is chosen to present a fair representation of the shape and size of the respective surface, similarly to the criterion for the function of Podolsky and Pauling (1929) in figure 1.

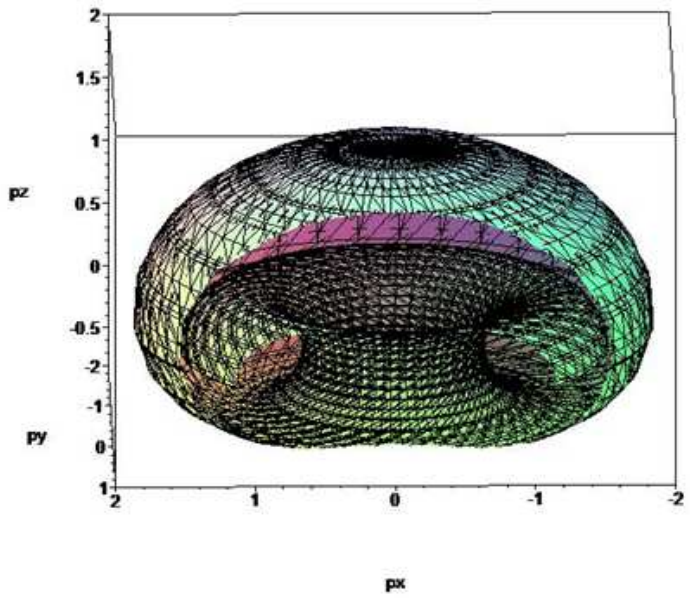

Figure 5. Surface of the real part of $\chi_{1,0,0}(\xi,\eta,\phi)$ showing an incomplete circular torus under a connected dome, cut open to show the internal structure; the axes are p_x, p_y and p_z.

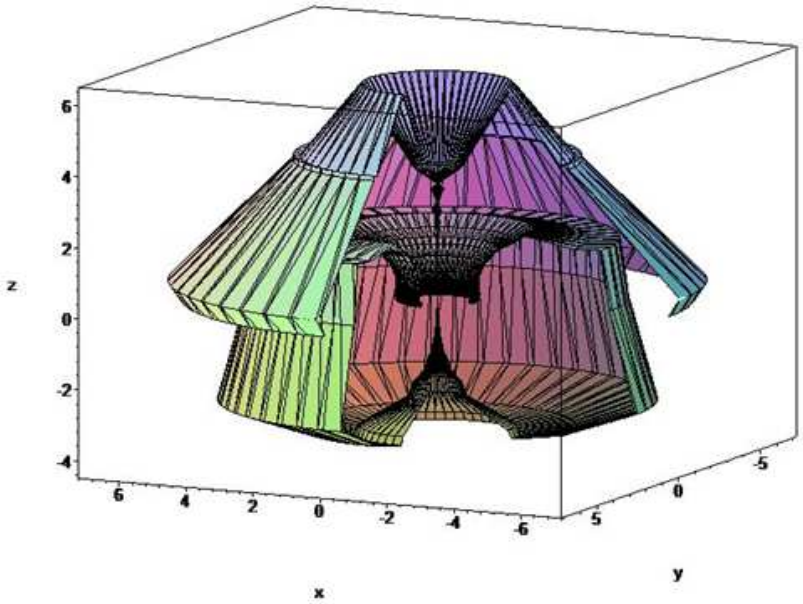

Figure 6. Surface of the imaginary part of $\chi_{1,0,0}(\xi,\eta,\phi)$, cut open to show the internal structure; the axes are p_x, p_y and p_z.

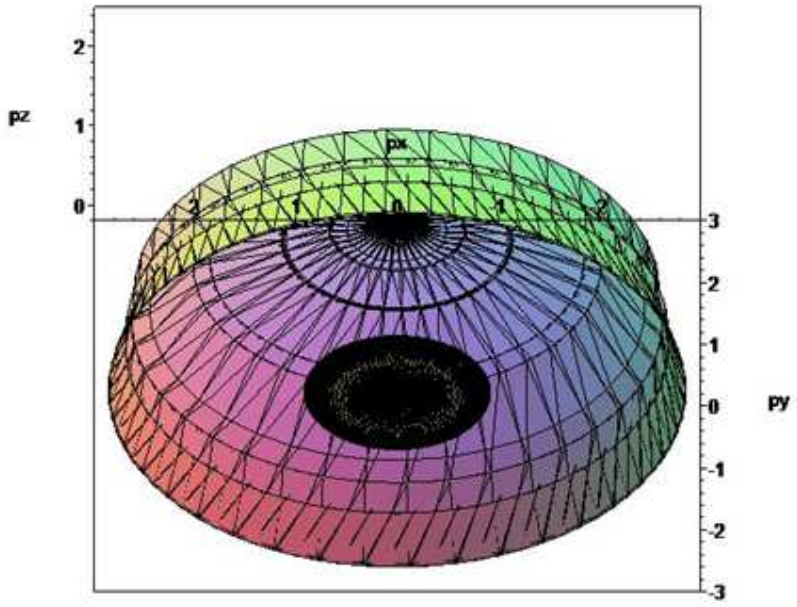

Figure 7. Surface of the square of $\chi_{1,0,0}(\xi,\eta,\phi)$, i.e. $|\chi_{1,0,0}|^2 = \chi_{1,0,0}{}^* \chi_{1,0,0}$; the axes are p_x, p_y and p_z.

Compared with the surfaces of amplitude functions in coordinate space, these surfaces of $\chi_{1,0,0}$ in momentum space exhibit astonishing properties. For instance, for the real part of $\chi_{1,0,0}$ an external view might seem to imply merely a circular torus with a nearly circular cross section, but cutting open the torus shows that two layers of surface exist for $p_z>0$, but only one layer for $p_z<0$. In contrast, the surface of the imaginary part of $\chi_{1,0,0}$ in figure 6 partly resembles a dome, such as for constant η in figure 3, but with angular rather than curved surfaces and some strange small structure along axis p_z; there is also a torus of a sort with angular rather than curved surfaces beneath the dome. In further contrast, the surface of $|\chi_{1,0,0}|^2$ in figure 7 closely resembles, but is not,

half a torus, sliced perpendicularly to axis p_z, at p_z=0; by its nature, this surface can not exist for p_z<0.

The surfaces of $\chi_{2,0,0}(\eta,\xi,\phi)$, of unnormalised formula,

$$\chi_{2,\,0,\,0}(\eta,\,\xi,\,\phi) = \frac{1\,\mathbf{e}^{(2\,i\,\xi)}\,(\cosh(\eta)-\cos(\xi))^2}{4\,\cosh(\eta)^4}$$

as the real and imaginary parts and its square are depicted in figures 8, 9, 10.

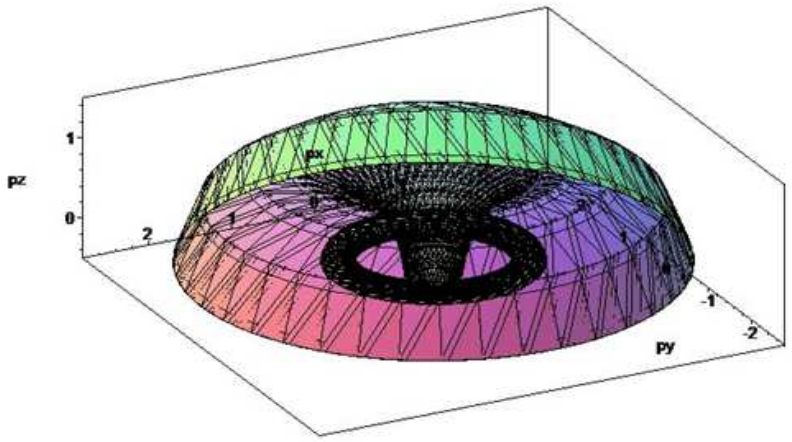

Figure 8. Surface of the real part of $\chi_{2,0,0}(\xi,\eta,\phi)$ showing part of a large dome above a small torus; the axes are p_x, p_y and p_z.

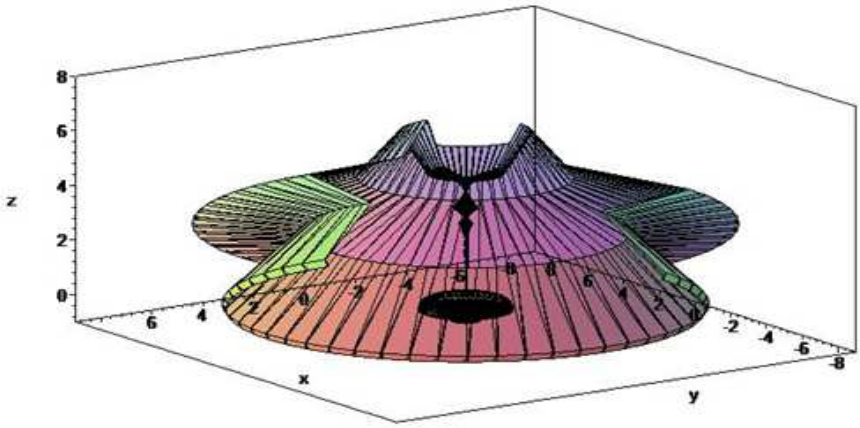

Figure 9. Surface of the imaginary part of $\chi_{2,0,0}(\xi,\eta,\phi)$, cut open to show the internal structure; the axes are p_x, p_y and p_z.

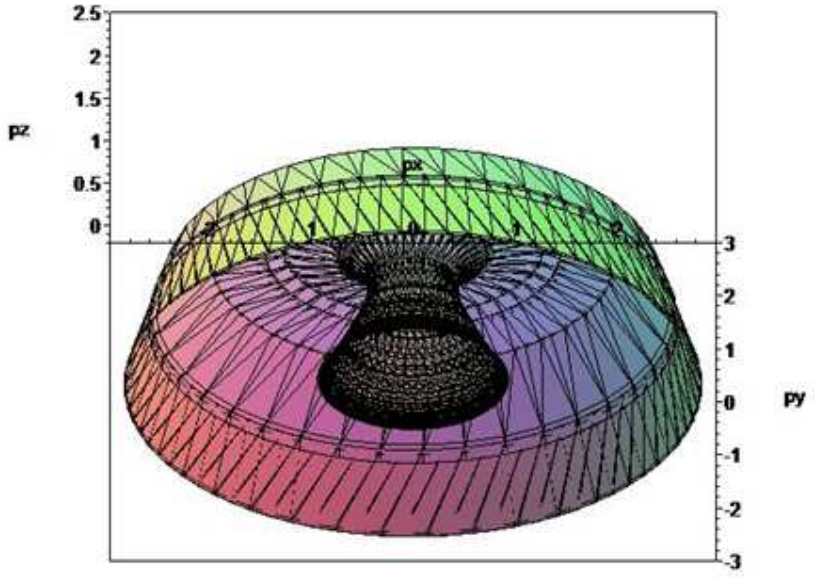

Figure 10. Total surface of the square of $\chi_{2,0,0}(\xi,\eta,\phi)$, i.e. $|\chi_{2,0,0}|^2 = \chi_{2,0,0^*}\,\chi_{2,0,0}$; the axes are p_x, p_y and p_z.

Comparison of figures 8, 9, 10 for $\chi_{2,0,0}(\xi,\eta,\phi)$ with the corresponding figures 5, 6, 7 for $\chi_{1,0,0}(\xi,\eta,\phi)$ indicates some evolution between these respective functions. For the real part of $\chi_{2,0,0}(\xi,\eta,\phi)$ a small torus replaces the large torus of $\chi_{1,0,0}(\xi,\eta,\phi)$ under a dome that has a circular shaft at its centre and that extends downward to the centre of the torus. For the imaginary part of $\chi_{2,0,0}(\xi,\eta,\phi)$, the gap between parts of the surface of $\chi_{1,0,0}(\xi,\eta,\phi)$ in figure 6 near the periphery exists no longer in figure 9, as the two sheets of the surface are visibly connected; a small torus near the base of the figure lies below some small structure along axis p_z. For $|\chi_{2,0,0}|^2$ in figure 10, the dome is opened along axis p_z to resemble an architectural oculus, namely a dome with a large opening at its centre and a cylindrical shaft protruding downward.

For $\chi_{2,1,0}(\xi,\eta,\phi)$, the surfaces of unnormalised formula,

$$\chi_{2,\,1,\,0}(\eta,\,\xi,\,\phi) = \frac{\mathbf{e}^{(2\,i\,\xi)}\,(\cosh(\eta)-\cos(\xi))^2}{\cosh(\eta)^6}$$

as its real and imaginary parts and its square are depicted in figures 11, 12, 13.

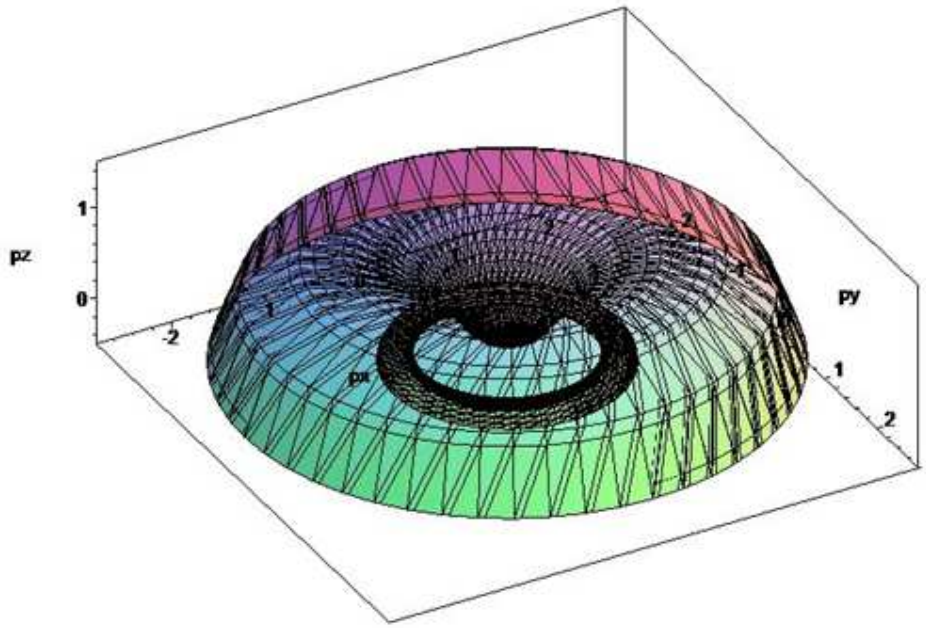

Figure 11. Surface of the real part of $\chi_{2,1,0}(\xi,\eta,\phi)$ showing part of a large dome above a small torus; the axes are p_x, p_y and p_z.

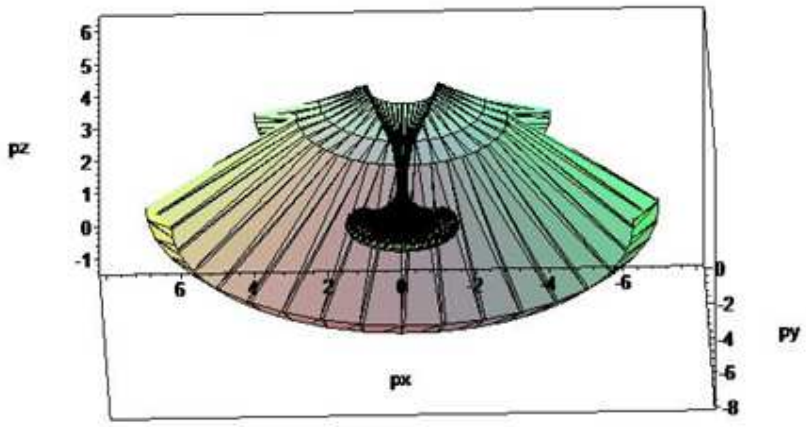

Figure 12. Surface of the imaginary part of $\chi_{2,1,0}(\xi,\eta,\phi)$, cut open to show the internal structure; the axes are p_x, p_y and p_z.

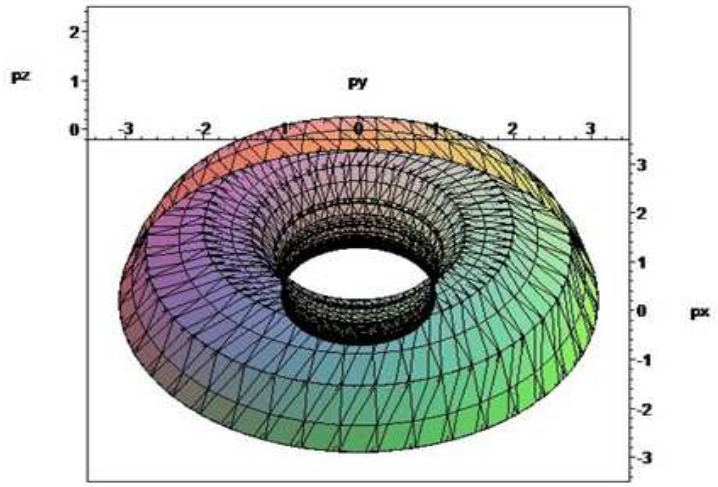

Figure 13. Total surface of the square of $\chi_{2,1,0}(\xi,\eta,\phi)$, i.e. $|\chi_{2,1,0}|^2 = \chi_{2,1,0^*}\,\chi_{2,1,0}$; the axes are p_x, p_y and p_z.

Of these surfaces pertaining to $\chi_{2,1,0}(\xi,\eta,\phi)$, the square $|\chi_{2,1,0}|^2$ is a perfect instance of an architectural oculus, whereas the real part has a torus under the closed area of an oculus; the imaginary part has angular outer features but a torus underneath them.

As a final instance of these momentum functions in toroidal space derived by Klein (1966), we present this function,

$$\chi_{3,\,2,\,0}(\eta,\,\xi,\,\phi) = -\frac{3}{8}\,\frac{\mathbf{e}^{(3\,i\,\xi)}\,(\cosh(\eta)^4 - 11)\,(\cosh(\eta) - \cos(\xi))^2}{\cosh(\eta)^9}$$

of which the surfaces of the real and imaginary parts and its square are displayed in figures 14, 15, 16, respectively.

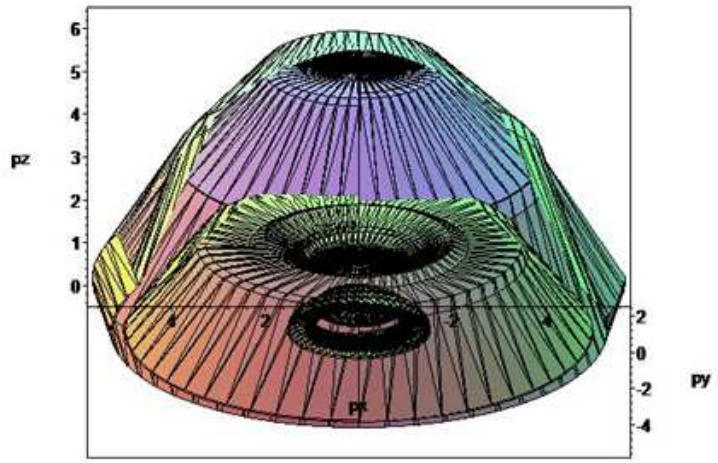

Figure 14. Surface of the real part of $\chi_{3,2,0}(\xi,\eta,\phi)$ cut open to show two small tori beneath an internal dome, under a further dome; the axes are p_x, p_y and p_z.

Figure 15. Surface of the imaginary part of $\chi_{3,2,0}(\xi,\eta,\phi)$, cut open to show the internal structure comprising a small torus under an angular dome; the axes p_x, p_y, p_z, omitted for clarity, have the same orientations as in figure 14; the axes are p_x, p_y and p_z.

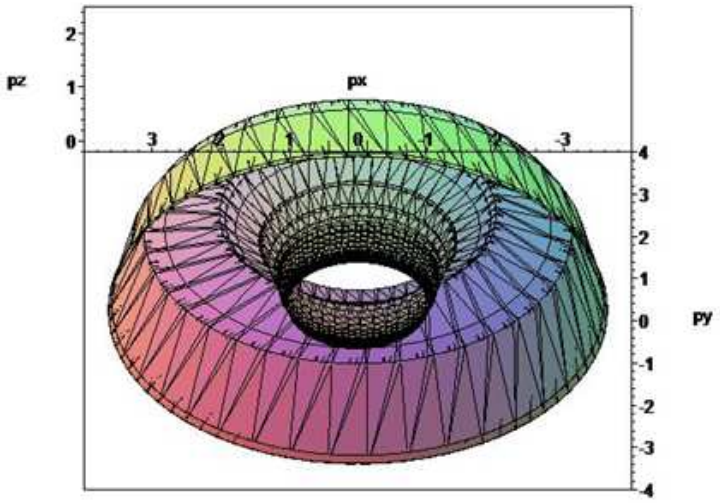

Figure 16. Total surface of the square of $\chi_{3,2,0}(\xi,\eta,\phi)$, i.e. $|\chi_{3,2,0}|^2 = \chi_{3,2,0^*}\,\chi_{3,2,0}$; the axes are p_x, p_y and p_z.

The shape of the surfaces of the squares of both $\chi_{2,1,0}(\xi,\eta,\phi)$ and $\chi_{3,2,0}(\xi,\eta,\phi)$ again resemble an architectural oculus. According to the same criterion for the chosen value of χ, the maximum diameter of $\chi_{3,2,0}(\xi,\eta,\phi)$ is slightly larger than that of $\chi_{2,1,0}(\xi,\eta,\phi)$. In contrast, the real part of $\chi_{3,2,0}(\xi,\eta,\phi)$ has no opening in its double dome and the imaginary part has only a small opening there. In all cases of these surfaces of toroidal momentum amplitude functions the surfaces are axially symmetric with respect to axis p_z.

IV. FUNCTIONS OF LOMBARDI

Lombardi (1980) recognised serious deficiencies in the derivation by Podolsky and Pauling (1929) of their amplitude functions in the momentum representation: their variables are not formed to be conjugate to any relevant spatial variables, so precluding a commutation relation with an appropriate spatial variable that leads to a Heisenberg relation of indeterminacy, and the angular coordinates are not chosen to be hermitian, which is a requirement of a quantum-mechanical system. Based not only on Podolsky's (1928) correct criteria but even more strongly on the work of De Witt (1952) who showed that, for any coordinate system, the conjugate momentum is the hermitian part of $p = \mathbf{i}\ \mathrm{d}/\mathrm{d}q$, for only cartesian coordinates does a direct Fourier transform of an

amplitude function in coordinate space produce a correct amplitude function in momentum space. Otherwise, for variables (q_1, q_2, …, q_n) in position space in n dimensions of any set, the volume element becomes $dV = g(q_1, q_2, \ldots, q_n)\, dq_1\, dq_2 \ldots dq_n$, in which $g(q_1, q_2, \ldots q_n)$ is the jacobian of the transformation between variables in the two sets. The most general transform between position space and momentum space is

$$\chi(p_1 \ldots p_n) = \frac{1}{2\pi\hbar}\int_{-\infty}^{\infty} S(p_1 \ldots p_n, q_1 \ldots q_n)\, \psi(q_1 \ldots q_n)\, g\, dq_1 \ldots dq_n$$

in which

$$S(p_1 \ldots p_n, q_1 \ldots q_n) = \frac{1}{\sqrt{g}} e^{-\left(i/\hbar\right)\boldsymbol{q}*\boldsymbol{p}}$$

The correct hermitian form of a momentum space variable is then

$$p_k \rightarrow -i\hbar\left(\frac{\partial}{\partial q_k} + \frac{1}{2g}\frac{\partial g}{\partial q_k}\right)$$

Lombardi (1980) considered three momentum variables (specified here as p_r, θ_p, ϕ_p), which were chosen to be conjugate to proper position variables (r, θ, ϕ) in spherical polar coordinates for the spatial amplitude function expressed as $\psi_{k,l,m}(r, \theta, \phi) = R(r)\, \Theta(\theta)\, \Phi(\phi)$. As the hydrogen atom is hence separable in the position representation in those coordinates, Lombardi transformed separately the radial equation and the angular equations, denoting the radial eigenfunctions in the momentum representation as $\alpha(p_r)$. Recalling that the eigenfunctions of the angular momentum operators, $\boldsymbol{L}^2$ and L_z, in position space are the spherical harmonics, $Y_{l,m}(\theta,\varphi)$, with eigenvalues $l(l+1)$ and m, respectively, he denoted the corresponding angular eigenfunctions in the momentum representation as $\beta(\theta_p)\, \rho(\phi_p)$. These functions must satisfy these expressions,

$$L^2\, \beta(\theta_p)\, \rho(\phi_p) = l(l+1)\, \hbar^2\, \beta(\theta_p)\, \rho(\phi_p)$$
$$L_z\, \rho(\phi_p) = m\, \hbar\, \rho(\phi_p)$$

The total momentum amplitude function for the hydrogen atom in momentum space was then written as

$$\chi(p_r, \theta_p, \phi_p) = \alpha(p_r)\, \beta(\theta_p)\, \rho(\phi_p)$$

For momentum space variable p_r, which is conjugate to position space radial variable r, the value of g for the transformation from $R(r)$ to $\alpha(p_r)$ is r^2. The resulting expression for the radial component was then derived to be

$$\alpha_{n,l}(p_r) = \frac{2^{(l+1)}\sqrt{\frac{n}{p_0}}\left(\sum_{k=0}^{n-l-1} \frac{\text{binomial}(n-l-1, k)\, 2^k\, (l+k+1)!\left(\frac{i\,p_0}{n\left(p_r - \frac{i\,p_0}{n}\right)}\right)^{(l+k+2)}}{(2\,l+k+1)!}\right)}{(n-l-1)!\sqrt{\pi\left(\sum_{k=0}^{n-l-1} \frac{\left(\sum_{j=0}^{n-l-1} \frac{(-1)^{(k+j)}\,(2\,l+k+j+2)!}{j!\,(n-l-j-1)!\,(2\,l+j+1)!}\right)}{k!\,(n-l-1-k)!\,(2\,l+k+1)!}\right)}}$$

This radial function is fully normalised for all n,l such that

$$\int_{-\infty}^{\infty} \alpha_{n,l}(p_r) * \alpha_{n,l}(p_r)\, dp_r = 1$$

The separation of variables yields an equation for ρ,

$$(\phi_p{}^2 - m^2\,\hbar^2)\;\rho(\phi_p) = 0$$

with the constant of separation chosen to be m^2, for which a simple solution,

$$\rho_m(\phi_p) = \delta(\phi_p \pm m\,\hbar)$$

contains Dirac delta function δ; m must be an integer (positive, negative or zero). This result is exactly as expected for a direct Fourier transform of coordinate function $\Phi(\phi) = \mathrm{e}^{(i\,m\,\phi)} / \sqrt{2\,\pi}$, as $g = 1$ for this ϕ dimension. The Dirac delta function is formally a distribution, not a true mathematical function; its square, or product with itself, is hence undefined. For this reason, a normalisation integral is impracticable -- i.e., unlike for $\alpha_{n,l}(p_r)$ above or $\beta_{l,m}(\theta_p)$ below, the quantity $\rho_m(\phi_p)$ as defined above is not square integrable.

With $g = \theta_p$ for the transformation from $\Theta(\theta)$, the solution of the equation for $\beta_{l,m}(\theta_p)$ is ultimately expressed, separately for $l - |m|$ = even integer,

$$\beta_{l,\,m}(\theta_p) = \sqrt{\frac{i\,(2\,l+1)\,(l-|m|)!}{2\,(l+|m|)!}}\;2^{|m|}\,\Gamma\!\left(\frac{1}{2}\right)\Gamma\!\left(\frac{|m|}{2}+1\right)\Gamma\!\left(\frac{|m|}{2}+\frac{1}{2}\right)\left(\frac{2}{\theta_p}\right)^{\left(\frac{|m|}{2}+\frac{1}{2}\right)}\Bigg($$
$$\sum_{k=0}^{\frac{l}{2}-\frac{|m|}{2}}\left(2\,k+\frac{|m|}{2}+\frac{1}{2}\right)(-i)^{(2\,k)}\,\mathrm{J}\!\left(2\,k+\frac{|m|}{2}+\frac{1}{2},\theta_p\right)\mathrm{ph}\!\left(-\frac{l}{2}+\frac{|m|}{2},k\right)$$
$$\mathrm{ph}\!\left(\frac{l}{2}+\frac{|m|}{2}+\frac{1}{2},k\right)(-1)^{\left(\frac{l}{2}-\frac{|m|}{2}-k\right)}\,\mathrm{ph}\!\left(\frac{|m|}{2},\frac{l}{2}-\frac{|m|}{2}-k\right)\mathrm{ph}\!\left(\frac{|m|}{2}+\frac{1}{2},k\right)$$
$$\mathrm{ph}\!\left(\frac{|m|}{2}+1,k\right)\Big/\left(k!\,\mathrm{ph}\!\left(\frac{1}{2},k\right)\mathrm{ph}\!\left(\frac{|m|}{2}+\frac{3}{2}+\frac{l}{2}-\frac{|m|}{2},k\right)\right)\Bigg)\Big/\Bigg($$
$$\Gamma\!\left(\frac{1}{2}-\frac{l}{2}-\frac{1\,|m|}{2}\right)\Gamma\!\left(1+\frac{l}{2}-\frac{|m|}{2}\right)\Gamma\!\left(\frac{3}{2}+\frac{l}{2}\right)\Bigg)$$

and for $l - |m|$ = odd integer;

$$\beta_{l,\,m}(\theta_p) = -\sqrt{\frac{i\,(2\,l+1)\,(l-|m|)!}{2\,(l+|m|)!}}\;2^{(|m|+1)}\,\Gamma\!\left(\frac{1}{2}\right)\Gamma\!\left(\frac{|m|}{2}+1\right)\Gamma\!\left(\frac{|m|}{2}+\frac{3}{2}\right)$$
$$\left(\frac{2}{\theta_p}\right)^{\left(\frac{|m|}{2}+\frac{1}{2}\right)}\Bigg(\sum_{k=0}^{\frac{l}{2}-\frac{|m|}{2}-\frac{1}{2}}\left(2\,k+\frac{|m|}{2}+\frac{3}{2}\right)(-i)^{(2\,k+1)}\,\mathrm{J}\!\left(2\,k+\frac{|m|}{2}+\frac{3}{2},\theta_p\right)$$
$$\mathrm{ph}\!\left(-\frac{l}{2}+\frac{|m|}{2}+\frac{1}{2},k\right)\mathrm{ph}\!\left(\frac{l}{2}+\frac{|m|}{2}+1,k\right)(-1)^{\left(\frac{l}{2}-\frac{|m|}{2}-\frac{1}{2}-k\right)}$$
$$\mathrm{ph}\!\left(\frac{|m|}{2},\frac{l}{2}-\frac{|m|}{2}-\frac{1}{2}-k\right)\mathrm{ph}\!\left(\frac{|m|}{2}+\frac{3}{2},k\right)\mathrm{ph}\!\left(\frac{|m|}{2}+1,k\right)\Big/\left(k!\,\mathrm{ph}\!\left(\frac{3}{2},k\right)\right.$$

These formulae that contain Bessel function J and Pochhammer function ph (here expressed as $\mathrm{ph}(x,y)$ but commonly written $(x)_y$, in either case equal to $\Gamma(x+y)/\Gamma(y)$), are fully normalised according to

$$\int_0^{\infty}\beta_{l,\,m}(\theta_p) * \beta_{l,\,m}(\theta_p)\,d\theta_p = 1$$

We present some plots of the squares of $\chi_{n,l,m}(p_r,\theta_p,\phi_p)$ without $\rho(\phi_p)$, i.e. $|\alpha_{n,l}(p_r)\ \beta_{l,m}(\theta_p)|^2$ because $\rho(\phi_p)$ as a Dirac δ function defies its incorporation into such a square that can yield a plot. We display first such a square of $\chi_{2,0,0}(p_r,\theta_p,\phi_p)$ without $\rho(\phi_p)$ is expressed with this formula,

$$\chi_{2,\,0,\,0}(p_r,\,\theta_p,\,\phi_p)\ = \alpha_{2,0}(p_r)\ \beta_{0,0}(\theta_p) = \frac{2\,(1+i)\,p_0^{\left(\frac{3}{2}\right)}\,(p_0\,i+2\,p_r)\,\sin(\theta_p)}{(p_0\,i-2\,p_r)^3\,\theta_p\,\pi}$$

of which the surface of the square appears in figure 17.

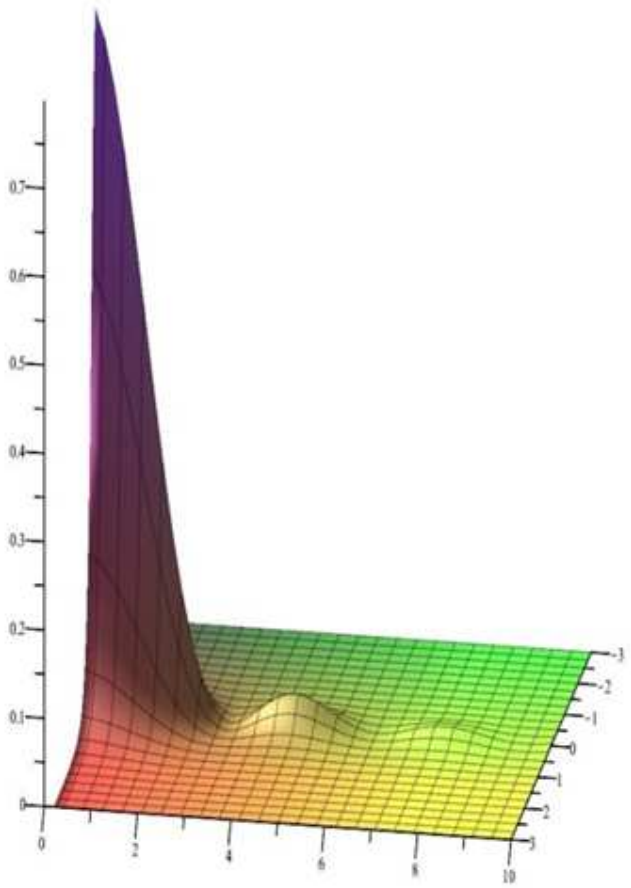

Figure 17. $|\alpha_{2,0}(p_r)\ \beta_{0,0}(\theta_p)|^2$ as a surface for $-3 < p_r/p_0 < 3$ and $0 < \theta_p < 10$

This surface exhibits a decreasing sequence of maxima along axis θ_p of which only three appear within the region for $0 < \theta_p < 10$, and of which the absolute maximum is at $\theta_p = 0$. The surface of $|\alpha_{1,0}(p_r)\ \beta_{0,0}(\theta_p)|^2$ is similar to that in figure 17 but the two subsidiary maxima are less prominent; correspondingly for $n > 2$, the sequence of subsidiary maxima along axis θ_p are increasingly prominent. In figure 18 is displayed the surface of $|\alpha_{2,1}(p_r)\ \beta_{1,0}(\theta_p)|^2$, according to this formula for $\chi_{2,1,0}(p_r,\theta_p,\phi_p)$ without the delta function containing ϕ_p.

$$\alpha_{2,1}(p_r)\ \beta_{1,0}(\theta_p) = \frac{-4\,(1+i)\,p_0^{\left(\frac{5}{2}\right)}\,(\cos(\theta_p)\,\theta_p-\sin(\theta_p))}{\theta_p^{\,2}\,\pi\,(p_0\,i-2\,p_r)^3}$$

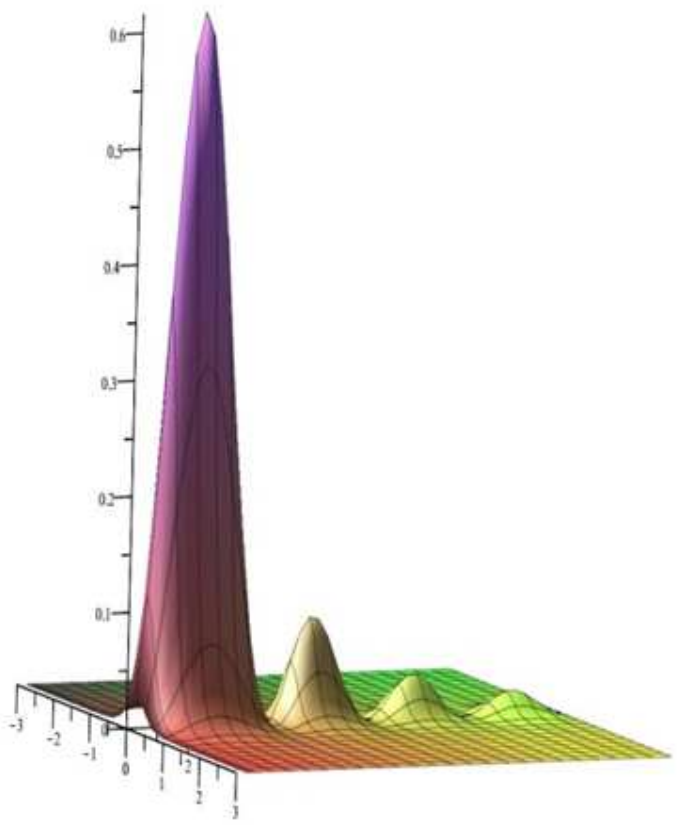

Figure 18. $|\alpha_{2,1}(p_r)\ \beta_{1,0}(\theta_p)|^2$ as a surface for $-3 < p_r/p_0 < 3$ and $0 < \theta_p < 13$

This surface of $|\alpha_{2,1}(p_r)\ \beta_{1,0}(\theta_p)|^2$ resembles the surface of $|\alpha_{2,0}(p_r)\ \beta_{0,0}(\theta_p)|^2$ except that the subsidiary maxima are here more prominent and the principal maximum is shifted to near θ_p=2. Other surfaces of $|\alpha_{n,l}(p_r)\ \beta_{l,m}(\theta_p)|^2$ have analogous characteristics.

Lombardi (2019) derived functions for the momentum amplitude of the hydrogen atom also for the momentum space related to the coordinate space in paraboloidal coordinates u,v,ϕ, defined in figure 19. In this coordinate system, the jacobian of the transformation is $(u, v) = ¼\ (u + v)^2$, which is not separable into a product of one-dimensional terms. Because of the symmetry between the two coordinates u and v, the resulting amplitude function in momentum space is expressible as

$$\chi_{n_1,\, n_2,\, m}(p_u, p_v, \phi_p) \;=\; \alpha_{n,\, n_u,\, l}(p_u)\ \ \alpha_{n,\, n_v,\, l}(p_v)\ \ \rho_m(\phi_p)$$

in which each α function has this form.

$$\alpha_{n,\, n_j,\, l}(p_j) = \; 2^{(l+1)} \sqrt{\frac{n}{p_0}} \left(\frac{\left(\frac{i\,p_0}{n\left(p_j - \frac{i\,p_0}{n}\right)} \right)^{(l+2)} \mathrm{hg}\left([\,l+2, -n_j+l+1\,], [\,2\,l+2\,], \frac{2\,i\,p_0}{i\,p_0 - n\,p_j} \right)}{\mathrm{ph}(l+2, l)} - \right.$$

$$\left. 2^{\mathrm{ce}(n_j - l)}\ \mathrm{ph}(n_j - l - \mathrm{ce}(n_j - l), \mathrm{ce}(n_j - l)) \left(\frac{i\,p_0}{n\left(p_j - \frac{i\,p_0}{n}\right)} \right)^{(l+2+\mathrm{ce}(n_j - l))} \mathrm{hg}\Big(\right.$$

$$[\,1, l+2+\mathrm{ce}(n_j - l), \mathrm{ce}(n_j - l) + l - n_j + 1\,], [\,1 + \mathrm{ce}(n_j - l), 2\,l + 2 + \mathrm{ce}(n_j - l)\,],$$

$$\left(\frac{2\,i\,p_0}{i\,p_0 - n\,p_j}\right) \Big/ (\mathrm{ce}(n_j - l)!\,\mathrm{ph}(l + 2 + \mathrm{ce}(n_j - l), l))\Bigg) \Big/ \Bigg(\Gamma(n_j - l)\left(\pi\left(\right.\right.\right.$$

$$\sum_{k=0}^{\mathrm{ce}(n_j - l) - 1} \left(\frac{(-1)^k\,(2\,l + k + 2)!\,\mathrm{hg}([2\,l + k + 3, -n_j + l + 1], [2\,l + 2], 1)}{\Gamma(n_j - l)\,(2\,l + 1)!} - \right.$$

$$(-1)^{(k + \mathrm{ce}(n_j - l))}\,(2\,l + k + \mathrm{ce}(n_j - l) + 2)!\,\mathrm{hg}($$

$$[1, \mathrm{ce}(n_j - l) + 2\,l + k + 3, \mathrm{ce}(n_j - l) + l - n_j + 1],$$

$$[1 + \mathrm{ce}(n_j - l), 2\,l + 2 + \mathrm{ce}(n_j - l)], 1) \Big/ (\mathrm{ce}(n_j - l)!\,\Gamma(n_j - l - \mathrm{ce}(n_j - l))$$

$$\left.\left.\left.\left.(2\,l + \mathrm{ce}(n_j - l) + 1)!)\right) \Big/ (\Gamma(n_j - l - k)\,k!\,(2\,l + k + 1)!)\right)\right)^{(1/2)}\right)$$

In this formula appear *ph* for a Pochhammer function, defined above, *hg* for a hypergeometric function and *ce* that denotes the ceiling or smallest integer greater than or equal to the number that is the argument of this function. Quantum number n pertains to energy and n_j, as n_1 or n_2, to momentum variable p_j as either p_u or p_v corresponding to coordinate variable either u or v, respectively. Also in this formula appears l as a dummy variable defined with $|m| = 2\,l + 1$, distinct from quantum number l in functions in spherical polar coordinates above; l assumes values of integer (for m even) and half integer (for m odd) because quantity $l\,(l + 1)$ of spherical polar coordinates is replaced with $(m^2 - 1)$ such that $n = n_1 + n_2 + |m| + 1$. The third factor in $\chi(p_u,p_v,\phi_p)$ has exactly the same form as in the transformation from spherical polar coordinates, explicitly,

$$\rho_m(\phi_p) = \delta(\phi_p \pm m\,\hbar)$$

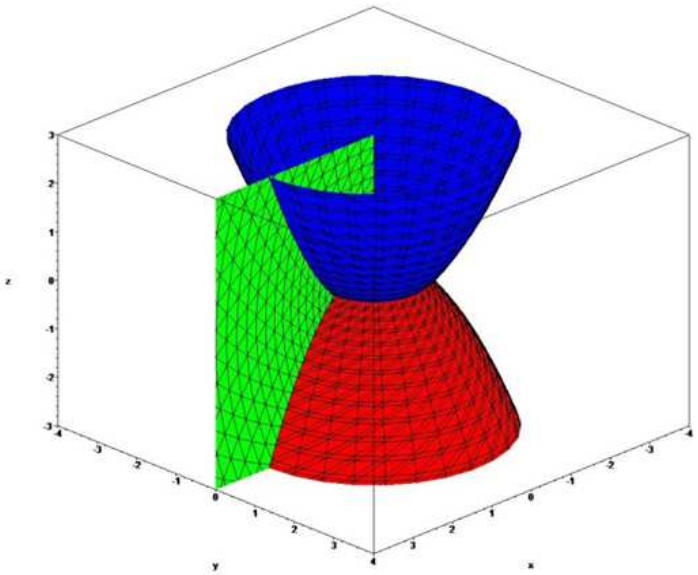

Figure 19. Surfaces of constant coordinates (u,v,ϕ) in the paraboloidal system; a surface for $u = 1$ is a red paraboloid opening downward; a surface for $v = 1$ is a blue paraboloid opening upward; a surface for $\phi = 0$ is a half-plane extending from the vertical symmetry axis.

We present some figures exhibiting surfaces of amplitude functions in momentum space transformed from amplitude functions in paraboloidal coordinates for selected values of n_1 and n_2 with $m = 0$, so without factor $\rho_m(\phi_p)$ of which the Dirac delta function is problematic for purposes of plotting; the plots are thus simply the product of two α functions, displaying how that product varies as a function of p_u and p_v. Although the above formula for $\alpha_{n,n1,l}(p_u)$ or the analogous $\alpha_{n,n2,l}(p_v)$ appears complicated, the actual formulae for particular values of n, n_1, n_2 and m have simple forms, as demonstrated below, and like the functions transformed from spherical polar coordinates above. The first function is for the ground state of the hydrogen atom, of which the pertinent product is

$$\alpha_{1,0,-\frac{1}{2}}(p_u)\,\alpha_{1,0,-\frac{1}{2}}(p_v) = \frac{i\,p_0\sqrt{\dfrac{p_0\,i-p_u}{p_0\,i-p_v}}}{2\,(p_0\,i-p_u)^2\,(p_0\,i-p_v)}$$

As this product is complex, the most meaningful plot depicts its square, presented in figure 20, which shows a surface with a single maximum value at the origin, and four-fold symmetry about an axis through the origin and perpendicular to the momentum axes, rather than cylindrical symmetry.

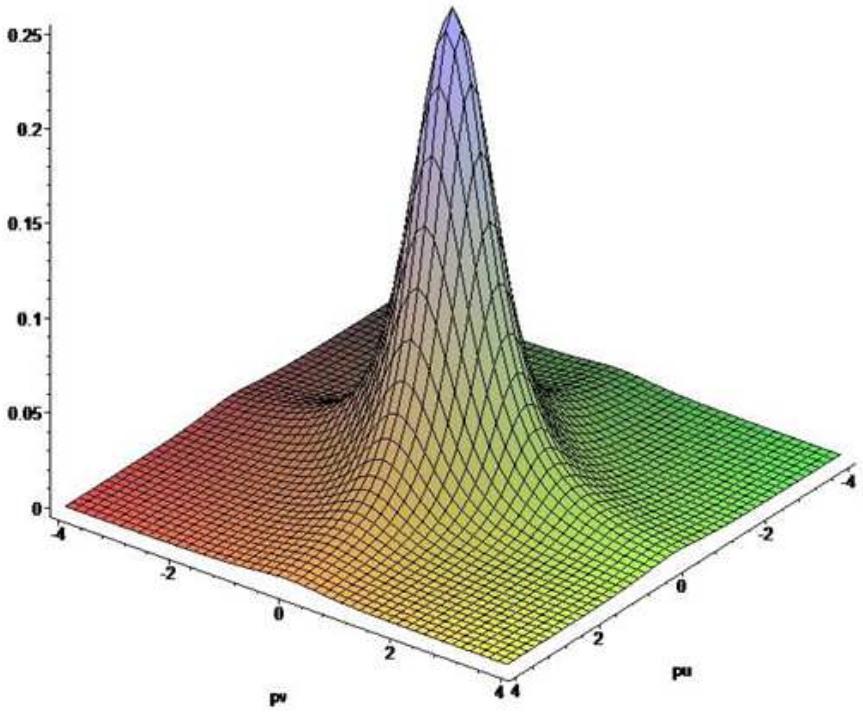

Figure 20. $\left|\alpha_{1,0,-\frac{1}{2}}(p_u)\,\alpha_{1,0,-\frac{1}{2}}(p_v)\right|^2$ as a function of momentum variables p_u/p_0 and p_v/p_0

Figure 21 presents an analogous plot of the square of a product of two α functions with disparate values of quantum numbers, $n_1 = 1$ and $n_2 = 0$; that product has this formula:

$$\alpha_{1,\,1,\,-\frac{1}{2}}(p_u)\,\alpha_{1,\,0,\,-\frac{1}{2}}(p_v) = -\frac{\sqrt{2}\;i\,{p_0}^2\,(p_0 I + 2\,p_u)\sqrt{\dfrac{p_0\,i - p_u}{p_0\,i - p_v}}}{4\,(p_0\,i - p_u)^3\,(p_0\,i - p_v)}$$

The surface of the square of this momentum amplitude function exhibits two maxima slightly displaced from the origin on either side along axis p_u, and a greater extension along this axis than along axis p_v. The analogous surface for a product with $n_1 = 0$ and $n_2 = 1$ shows also two maxima slightly displaced from the origin but on either side along axis p_v, as expected.

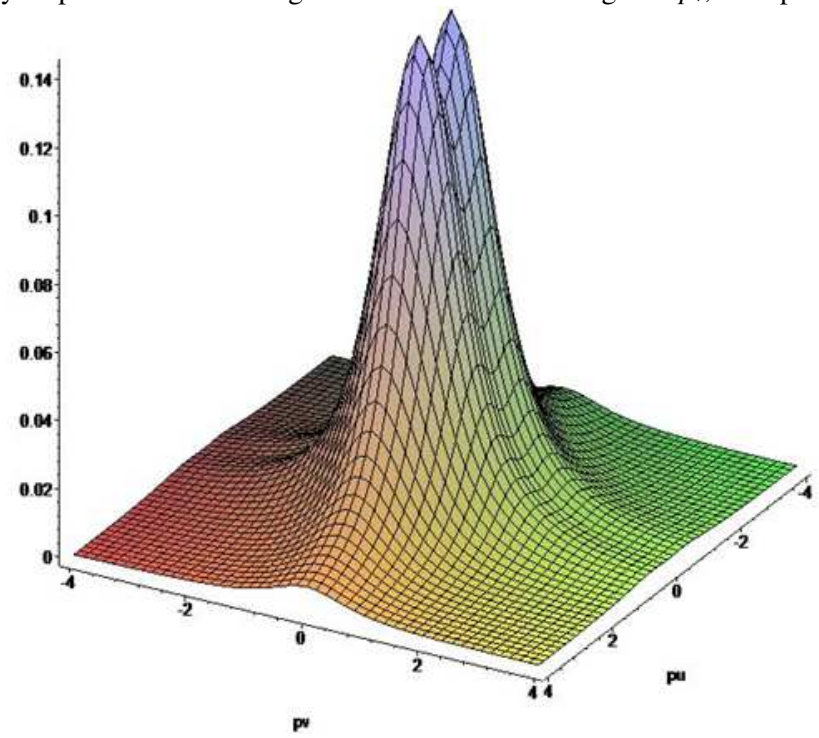

Figure 21. $\left|\alpha_{1,\,1,\,-\frac{1}{2}}(p_u)\,\alpha_{1,\,0,\,-\frac{1}{2}}(p_v)\right|^2$ as a function of momentum variables p_u/p_0 and p_v/p_0

Figure 22 presents an analogous plot of the square of a product of two α functions with quantum numbers at equal values, $n_1 = 1$ and $n_2 = 1$, according to this formula:

$$\alpha_{1,\,1,\,-\frac{1}{2}}(p_u)\,\alpha_{1,\,1,\,-\frac{1}{2}}(p_v) = \frac{i\,{p_0}^2\,(i\,p_0 + 2\,p_u)\sqrt{\dfrac{i\,p_0 - p_u}{i\,p_0 - p_v}}\,(i\,p_0 + 2\,p_v)}{4\,(i\,p_0 - p_u)^3\,(i\,p_0 - p_v)^2}$$

The surface of the square of this momentum amplitude function exhibits four maxima, each slightly displaced from the origin on either side along axis p_u and axis p_v, and a similar extension along both axes.

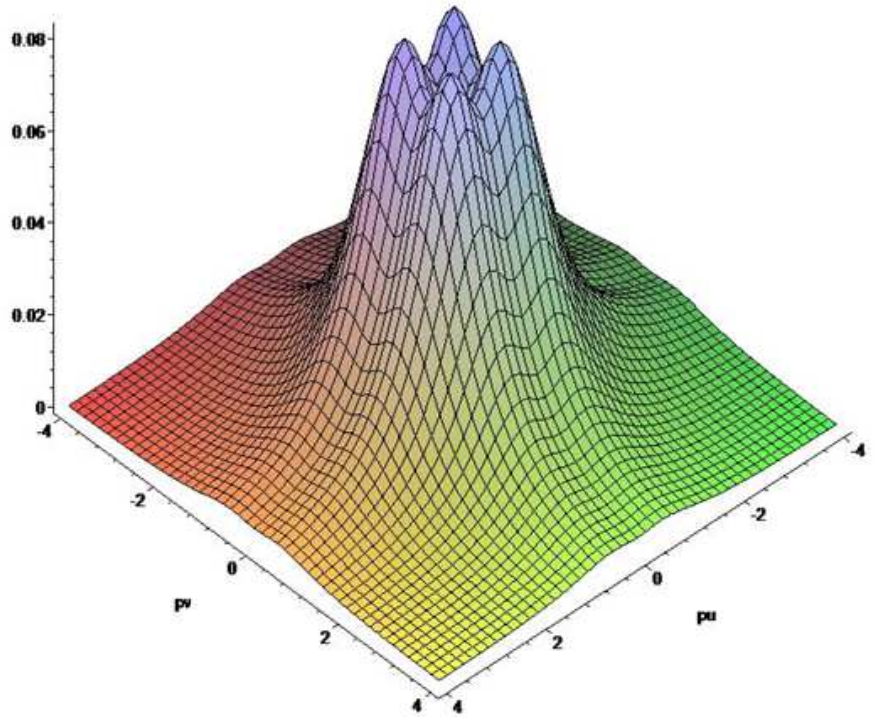

Figure 22. $\left| \alpha_{1,\,1,\,-\frac{1}{2}}(p_u)\,\alpha_{1,\,1,\,-\frac{1}{2}}(p_v) \right|^2$ as a function of momentum variables p_u/p_0 and p_v/p_0

Plots of squares of products $\alpha(p_u)\ \alpha(p_v)$ of other amplitude functions with $m = 0$ appear to have either one or two maxima, either one at the origin or two slightly displaced from the origin, along each axis p_u or p_v, independent of the values of n and n_1 or n_2. As n increases, the width of the curved surfaces becomes increasingly smaller and hence with increasing maximum squared amplitude at or near the origin.

V. DISCUSSION

These four amplitude functions for the hydrogen atom in the momentum representation -- those of Podolsky and Pauling (1929), apparently reproduced by Hylleraas (1932) and by Fock (1935), of Klein (1966) and of Lombardi (1980, 2020) in two systems -- comprise all such sets of known functions that have been fully characterised. A direct comparison of the plotted shapes of the surfaces in the various figures is meaningful only between the functions of Podolsky and Pauling transformed from spherical polar coordinates and of Klein transformed apparently from paraboloidal coordinates, or between the functions of Lombardi transformed from spherical polar coordinates and from paraboloidal coordinates. In each case the functions have disparate variables, even though in the plots the variables become displayed apparently in conventional cartesian momentum coordinates.

An essential ramification of the existence and quantitative definition of these multiple functions within the momentum representation is that they are all artefacts of both a particular method of quantum mechanics, specifically wave mechanics, and a particular momentum representation within wave mechanics. For a particular purpose of a calculation involving this method, functions in one set of momentum variables might prove more convenient than in another set of momentum variables, or than in one or other set of coordinate variables. The functions of Podolsky and Pauling (1929) are, however, deprecated for all purposes because they are incorrect;

although they result from a correct solution of the Schroedinger equation in coordinate space, its improper transformation into momentum variables makes their applicability generally worthless. For the same reason the functions of Hylleraas (1932) and Fock (1935), despite the skill of their derivations, suffer from the same fundamental deficiency, which those authors failed to recognise. For the functions of Klein (1966), that author admitted that whether his toroidal system would be useful for calculations is unclear, but their pedagogical value emphasises the presence of the Coulomb degeneracy in the hydrogen atom. The functions of Lombardi (1980, 2020) transformed from both spherical polar and paraboloidal coordinates are satisfactorily derived and well defined; the presence in each case of the questionable Dirac delta functions hinders plots of the surfaces of these functions at a selected value of amplitude χ, as is practicable for all amplitude functions in coordinate space at a selected value of amplitude ψ (Ogilvie, 2016), but might not impede calculations of properties of the hydrogen atom: for particular values of the pertinent quantum numbers, Lombardi's functions have no more complicated nature than the corresponding functions in coordinate space.

VI. CONCLUSION

How many separate sets of momentum amplitude functions are possible? In principle, for each set of coordinate amplitude functions there might exist a corresponding set of momentum functions, implying four such sets; other means of generating a momentum function can not be excluded. The present plots of amplitude functions, in four sets, in momentum variables in their real and imaginary parts and as their squares, presented in the various figures above, are available for comparison with plots of surfaces of amplitude functions in coordinate variables in four sets, reported previously (Ogilvie, 2016). The momentum amplitude functions in four sets here, however, claim their origins in only two sets of the amplitude functions in coordinate variables. These amplitude functions in momentum variables combined with the various amplitude functions in coordinate variables constitute at present a complete inventory of amplitude functions for the hydrogen atom as solutions to the Schroedinger equation.

VII. REFERENCES

De Witt, B. S. 1952. Point transformations in quantum mechanics, *Physical Review*, *85* (*4*), 653-661

Fock, V. 1935. Zur theorie des wasserstoffatoms, *Zeitschrift fuer Physik*, *98* (*1*), 145-154

Hylleraas, A. 1932. Zur wellengleichung des Keplerproblems im impulsraume, *Zeitschrift fuer Physik*, *74*, 216-224

Kalnins, E. G., Miller, W., Winternitz, P. 1976. The group O_4, separation of variables and the hydrogen atom, *SIAM Journal of Applied Mathematics*, *30*, 630 - 664

Klein, J. J. 1966. Eigenfunctions of the hydrogen atom in momentum space, *American Journal of Physics*, 34, 1039-1042

Lombardi, J. R. 1980. Hydrogen atom in the momentum representation, *Physical Review*, *22* (3), 797-802

Lombardi, J. R. 2020. The momentum representation of the hydrogen atom in paraboloidal coordinates, *Chemical Physics, 530*, 110636; arxiv 1906:02375 at https://arxiv.org

Ogilvie, J. F. 2016. The hydrogen atom -- wave mechanics beyond Schroedinger: orbitals as algebraic formulae derived in all four coordinate systems, *Ciencia y Tecnología*, *32* (*1*), 1-24

Podolsky, B. 1928. Quantum-mechanically correct form of hamiltonian function for conservative systems, *Physical Review*, *32* (*5*), 812-816

Podolsky, B., Pauling, L. C. 1929. The momentum distribution in hydrogen-like atoms, *Physical Review*, *34* (*1*), 109-116

Schroedinger, E. 1926. reprinted as *Collected papers on wave mechanics, together with his four lectures on wave mechanics*, third edition augmented, 2010, AMS Chelsea, Providence, RI USA

Weyl, H. 1927. Quantenmechanik und gruppentheorie, *Zeitschrift fuer Physik*, *46* (*1*), 1-46